Monatshefte für Chemie 132, 1279–1294 (2001)

Monatshefte für Chemie
Chemical Monthly

Printed in Austria

Invited Review

Thermochromism and Solvatochromism in Solution

Usama El-Ayaan[1,2], **Fumiko Murata**[2], and **Yutaka Fukuda**[2,*]

[1] Department of Chemistry, Faculty of Science, Mansoura University, Mansoura 35516, Egypt
[2] Department of Chemistry, Faculty of Science, Ochanomizu University, Tokyo 112-8610, Japan

Summary. The thermochromic behaviour of various coordination compounds in solution is discussed, with a special focus on cyclic diamine chelates. Thermally induced spin-crossover phenomena of iron(II) complexes are also considered. The solvatochromic behaviour of mixed-ligand complexes is presented in detail.

Keywords. Thermochromism; Spin-crossover; Solvatochromism; Solvent effect; Magnetic properties.

Introduction

The colours of coordination compounds originate from (*i*) d–d transitions, (*ii*) CT transitions (*ML*- and *LM*-CT), (*iii*) intervalence transitions, and (*iv*) ligand π–π^* transitions. The change of chemical and physical conditions (temperature, pressure, solvent, *etc.*) strongly influences the colours of the complexes. Colour change induced by temperature is known as thermochromism. Solvatochromism is another property of many coordination compounds; in this case, colour change is a consequence of solvent polarity.

Thermochromism

The term thermochromism is defined as the change of the colour of a substance, or a system of substances, when heated to a certain temperature. The change can be reversible, *i.e.* the original colour returns upon cooling, or irreversible.

Thermochromism on thermally induced spin-crossover iron(II) complexes

Thermally induced spin-state transitions between the low-spin (LS) and the high-spin (HS) states of transition metal complexes with d^4 to d^7 electronic configuration are observed when the ligand field splitting energy ($\Delta_0 = 10\,\mathrm{Dq}$) is approximately

---

* Corresponding author. E-mail: usama@cc.ocha.ac.jp

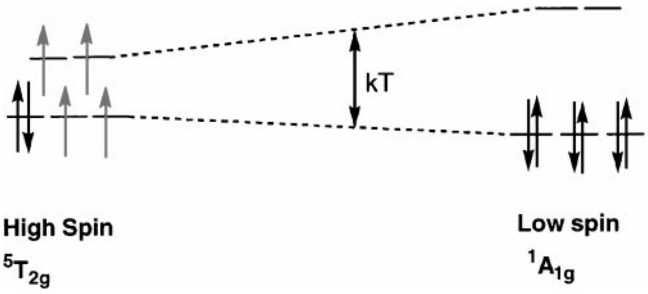

Fig. 1. High-spin and low-spin states in iron(II) compounds

outweighed by the spin-pairing energy P [1, 2]. In other words, a spin-crossover phenomenon is observed when the energy difference between the HS and LS states is of the order of kT (Fig. 1). In the course of such a spin-crossover, temperature dependent changes of the magnetic moment are observed.

A thermally induced LS $\leftrightarrows$ HS transition is characterized by an $x = f(T)$ curve, where x is the molar fraction of HS molecules and $(1 - x)$ that of LS molecules. A method to obtain such a curve is to measure the temperature dependence of the magnetic susceptibility. χT is constant in the temperature range where all molecules are in the same spin state ($(\chi T)_{\mathrm{LS}}$ and $(\chi T)_{\mathrm{HS}}$, respectively). Therefore, the $x = f(T)$ curve can be deduced from the experimental $\chi T = f(T)$ curve according to Eq. (1).

$$x = \chi T - (\chi T)_{\mathrm{LS}}/(\chi T)_{\mathrm{HS}} - (\chi T)_{\mathrm{LS}} \qquad (1)$$

Spin-crossover phenomena ($S = 0$ to $S = 2$ transitions) have been well documented for various iron(II) complexes [3, 4]. Among them, [Fe(*phen*)$_2$(NCS)$_2$], [Fe(*phen*)$_2$(NCSe)$_2$], and [Fe(*bpy*)$_2$(NCS)$_2$] have been studied using different experimental techniques. It should be pointed out that [Fe(*phen*)$_3$]$X_2 \cdot n$H$_2$O complexes keep their spin state unchanged when the temperature is varied, *i.e.* without showing any spin-crossover phenomena. They are either of low-spin ($^1A_1, S = 0$), intermediate-spin ($^3T_1, S = 1$), or high-spin ($^5T_2, S = 2$) nature [5]. Generally, some asymmetry in the ligand field sphere can produce an appropriate balance between the ligand field strength and the spin pairing energy, thus leading to the conditions necessary for the spin-crossover.

The Fe(II) complex [Fe(*ptz*)$_6$](BF$_4$)$_2$ (Fig. 2; *ptz* = 1-propyltetrazole) is known to exhibit a spin transition at 135 K with a spectacular change of colour from purple (LS) to white (HS) [6, 7]. Its UV/Vis spectrum at room temperature is typical of a $^5T_{2g}$ ground state with a $^5T_{2g} \leftrightarrows {}^5E_g$ spin-allowed transition at 12250 cm^{-1}, whereas that at 10 K corresponds to a $^1A_{1g}$ ground state with $^1A_{1g} \rightarrow {}^1T_{1g}$ and $^1A_{1g} \rightarrow {}^1T_{2g}$ spin-allowed transitions at 18400 and 26700 cm^{-1}.

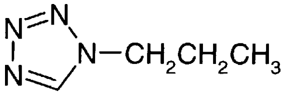

Fig. 2. Structure of 1-propyltetrazole

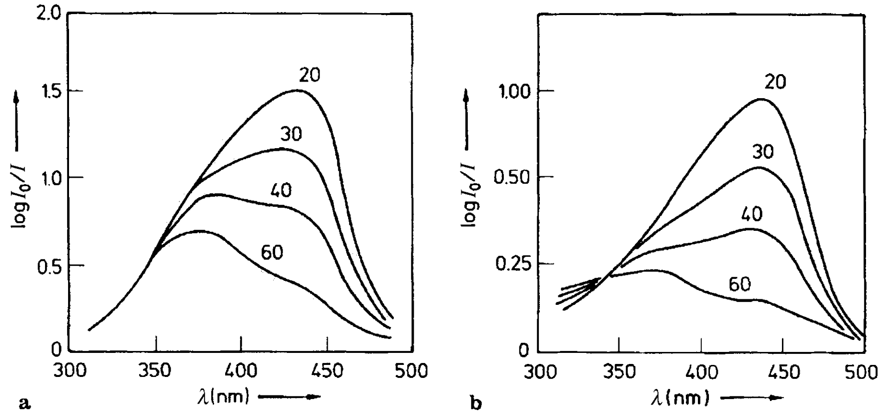

Fig. 3. Absorption spectra of $[Fe(amp)_3]^{2+}$ at different temperatures; (a) $4 \times 10^{-4}\,M$ in CH_3CN/H_2O, (b) $1.9 \times 10^{-4}\,M$ in H_2O; the temperature (°C) is given on each curve

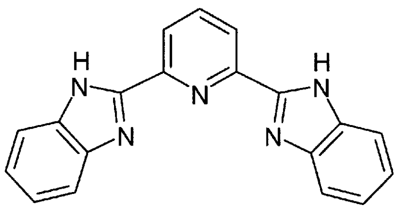

Fig. 4. Structure of 2,6-*bis*-(benzimidazol-2′-yl)-pyridine

Temperature-dependent electronic spectra of $[Fe(amp)_3]^{2+}$ (*amp* = 2-amino-methyl-pyridine) exhibit two intense absorption bands at 440 and 380 nm in water or water/acetonitrile [8]. The relative intensities of these bands change sharply with temperature (Fig. 3).

The iron(II) complex $[Fe(bzimpy)_2](ClO_4)_2$ (Fig. 4; *bzimpy* = 2,6-*bis*-(benzimidazol-2′-yl)-pyridine) has been shown to exhibit a pronounced spin-crossover $({}^1A_{1g}(O_h) \leftrightarrows {}^5T_{2g}(O_h))$ in solution [9].

Temperature-dependent UV/Vis spectroscopic measurements of $[Fe(bzimpy)_2](ClO_4)_2$ in ethanol:methanol = 1:1 from 300 down to 15 K and in a polyvinyl alcohol (*PVA*) matrix have been carried out [10]. The CT bands located in the region of 316–362 nm were found to be sensitive to the spin transition (Fig. 5). Upon cooling they increase in intensity because of the higher extinction coefficient in the low-spin species due to π-back donation. Also, the peak located at 570 nm shows both LS and HS properties [11]. The increase in intensity upon cooling indicates a raising amount of LS, *i.e.* the extinction of the LS state is higher (Fig. 5).

4-*X*-2,6-*bis*-(benzimidazol-2′-yl)-pyridine (*X* = H, Cl, OH) can coordinate as a tridentate ligand to metal ions of d^4–d^7 electronic configuration in distorted octahedral geometry [12, 13]. Among these complexes, $[Fe(X\text{-}bzimpy)_2]^{2+}$ exhibits a pronounced spin-crossover behaviour both in solution and in the solid state [14, 15]. Thermally induced spin-crossover in solution has been observed in

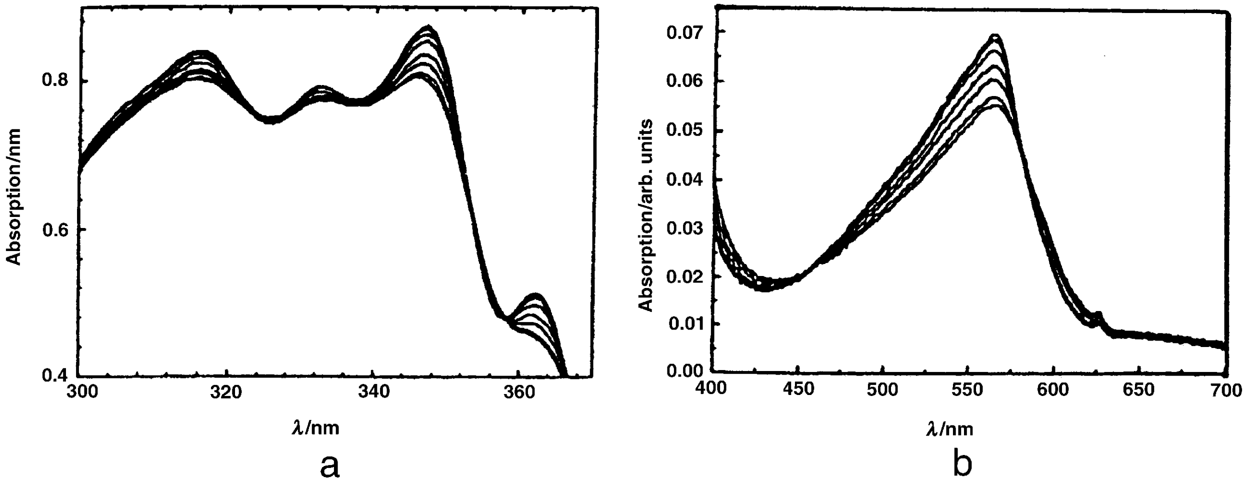

Fig. 5. Temperature dependent UV/Vis spectra of $[Fe(\mathit{bzimpy})_2](ClO_4)_2$ in *PVA* in the wavelength ranges (a) 300–370 and (b) 400–700 nm; temperatures (K) from bottom to top: 300, 265, 225, 195, 150, 100, 50, 15

Table 1. Magnetic parameters of $[Fe(X\text{-}\mathit{bzimpy})_2]^{2+}$ and $[Fe(H\text{-}\mathit{bzimpy}H_{-1})_2]$ in MeOH and thermodynamic parameters derived thereof

T/K	$[Fe(H\text{-}\mathit{bzimpy})_2]^{2+}$		$[Fe(H\text{-}\mathit{bzimpy}H_{-1})_2]$	
	μ/μ_B	K_{sc}	μ/μ_B	K_{sc}
240	2.32	0.22	1.65	0.10
250	3.14	0.48	2.62	0.29
260	3.63	0.77	3.21	0.52
270	4.12	1.28	3.70	0.83
280	4.36	1.69	4.18	1.37
290	4.62	2.40	4.44	1.87
300	4.82	3.31	4.52	2.08
310	4.95	4.26	4.78	3.09
320	5.03	5.11	5.03	5.11
ΔH (kJ/mol)	2.77 ± 0.6		25.6 ± 1.2	
ΔS (J/K · mol)	85.1 ± 2.1		92.8 ± 4.3	

$[Fe(H\text{-}\mathit{bzimpy})_2]^{2+}$ and its deprotonated form $[Fe(H\text{-}\mathit{bzimpy}H_{-1})_2]$ [16]. The magnetic moments of both complexes in methanolic solution were derived by applying the *Evans* method [17] at different temperatures (Table 1).

$[Fe(\mathit{pybzim})_3]X_2 \cdot nH_2O$ (Fig. 6; *pybzim* = 2-(2′-pyridyl)-benzimidazol) is a spin-crossover system which has been studied by various techniques [18–21]. NMR measurements on the perchlorate complex $[Fe(\mathit{pybzim})_3](ClO_4)_2 \cdot H_2O$ at different temperatures in methanol, acetonitrile, acetone, nitromethane, and dimethylsulfoxide have been reported (Table 2) [22]. The temperature dependence of the effective magnetic moment (evaluated by the *Evans* method) allows to conclude that spin-crossover occurs in these solutions.

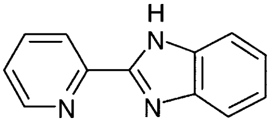

Fig. 6. Structure of 2-(2′-pyridyl)-benzimidazole

Table 2. Temperature dependent magnetic moments of $[\mathrm{Fe}(pybzim)_3](\mathrm{ClO}_4)_2 \cdot \mathrm{H_2O}$ in various solvents using *Evans*' method

T/K	μ/μ_B				
	MeOH	*Ac*	*AN*	*NM*	*DMSO*
325	–	–	–	–	5.37
320	4.74	4.96	3.56	4.76	5.33
315	–	–	–	–	5.29
310	4.83	4.95	3.24	4.69	5.24
300	4.90	4.87	3.19	4.44	
290	4.80	4.79	3.13	4.36	
280	4.68	4.71	3.08	3.94	
270	4.57	4.46	3.02	3.88	
260	4.45	4.20			
250	4.19	3.56			
240	3.92	2.85			
230	3.64	1.97			
220	3.21	1.60			

In methanol, the spin transition occurs at 220 K and culminates at 300 K. Even better resolution of the spin-crossover was observed in acetone. In contrast, in acetonitrile only a small variation of the effective magnetic moment was recorded from 270 to 320 K. In nitromethane and dimethylsulfoxide, only the high-spin state is stabilized within the accessible temperature range.

It is interesting to note that in the solid state the spin-crossover behaviour of such complexes varies remarkably with the counter anion, *e.g.* $X = \mathrm{BPh_4^-}$, $\mathrm{BF_4^-}$, $\mathrm{PF_6^-}$, $\mathrm{NO_3^-}$, $\mathrm{Br^-}$, $\mathrm{I^-}$, and $\mathrm{ClO_4^-}$ [23–25]. Also, the conditions of the preparation may cause different magnetic properties [26]. Additionally, in solution the nature of the solvent affects the spin transition [27].

Potential applications of thermally induced spin-crossover materials

Smart materials respond to their environment as *e.g.* illustrated by photochromic eyeglasses which darken upon exposure to ultraviolet light. Hence, materials with fast reversible responses to environmental stimuli are sought as components of smart systems. Similar to photochromic materials, thermochromic materials reversibly respond to heat and exhibit substantial colour changes upon small temperature variations. Spin-crossover materials are a class of thermochromic materials exhibiting fast and reversible colour changes amenable to display, memory, and switching devices. These colour changes also can be induced by light (photochromism) or pressure (piezochromism). Due to the nature of the mechanism of the thermo-, photo-, or piezochromic responses (*i.e.* redistribution of the electron density at a metal ion site within the molecule), in addition to reversibility these changes occur extremely fast. As a consequence of their favourable properties (fast colour change, strong contrast between colours, long-term colour stability, and lack of moving parts), these materials are completely recyclable and amenable to fast, low power-consuming, high data density display and storage devices for future systems [28].

Thermochromism of cyclic diamine complexes

In the solid state, cyclic diamine complexes are known to exhibit thermochromism. For example, the orange complex $[\mathrm{Cu}(\mathit{daco})_2](\mathrm{NO}_3)_2$ (*daco* = 1,5-diazacyclooctane) with a square-planar geometry around the copper(II) centre shows a reversible thermochromism. When heated above *ca.* 90°C the colour changes quite abruptly from orange to violet. Upon cooling, it gradually becomes orange again [29]. These observations can be explained by the hydrogen-bond breaking and reforming between the ligand amino proton and the nitrate anion.

In solution, thermochromism of Ni complexes with cyclic diamines is also interesting. In aqueous solution, the nickel(II) complex $[\mathrm{Ni}(\mathit{dachda})(\mathrm{OH}_2)_2]$ (*dachda* = 1,4-diazacycloheptanediacetate) and its alkyl derivatives (Fig. 7) show a pronounced thermochromism [30].

In case of the *dachda* complex, heating shifts the equilibrium of Eq. (2) to the right, resulting in a change of the geometry around the nickel(II) centre from octahedral to square-planar.

$$\underset{\text{green (room temp)}}{[\mathrm{Ni}(\mathit{dachda})(\mathrm{H_2O})_2]} \leftrightarrows \underset{\text{orange (high temp)}}{[\mathrm{Ni}(\mathit{dachda})]} + 2\mathrm{H_2O} \qquad (2)$$

The UV/Vis spectra of $[\mathrm{Ni}(\mathit{dachda})(\mathrm{H_2O})_2]$ at different temperatures show that the peak intensity at $21 \times 10^3\,\mathrm{cm}^{-1}$ gradually increases as the temperature increases (Fig. 8), favouring the square-planar structure.

In case of all other Ni complexes discussed, the equilibrium is shifted from a 5-coordinated to a square-planar geometry (Eq. (3)); in other words, the alkyl substituent stabilizes the planar species, so that the thermochromic change involving

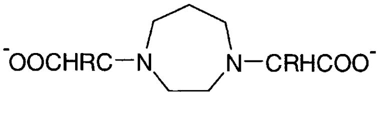

R	Abbreviation
H	*dachda*
Me	*dachdma*
Et	*dachdea*
n-Pr	*dachdpa*

Fig. 7. Structure of 1,4-diazacycloheptanedicarboxylate

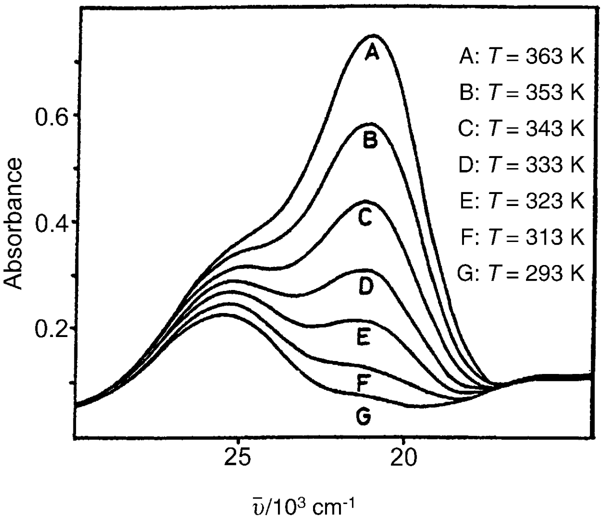

Fig. 8. Electronic absorption spectra of [Ni(*dachda*)(H_2O)$_2$] at different temperatures (2.3×10^{-2} *M* in H_2O)

its formation by heating occurs at much lower temperatures than for the *dachda* complex.

$$\underset{\text{5-coordinated}}{[\mathrm{Ni}(\mathit{dachdRa})(\mathrm{H_2O})]} \underset{\text{cool}}{\overset{\text{heat}}{\rightleftharpoons}} \underset{\text{square-planar}}{[\mathrm{Ni}(\mathit{dachdRa})]} + \mathrm{H_2O} \tag{3}$$

It is interesting to note that when a large excess of $NaClO_4$ is added to a green solution of [Ni(*dachda*)(H_2O)$_2$], the colour changes from green to orange at room temperature. This effect of colour change induced by $NaClO_4$ addition is known as the inert salt effect and is explained by decreasing the coordination ability of the free water molecules due to the presence of a large amount of the inert salt in solution. The addition of $NaClO_4$ is sometimes important to improve thermochromism, like in the case of [Ni(*diam*)$_2$(H_2O)$_2$]$^{2+}$ (*diam* = ethylenediamine or propylenediamine). Although the ethanolic solution of this complex is thermochromic and changes its colour reversibly from blue-violet to orange upon heating (Eq. (4)), the aqueous solution is not [31].

$$\underset{\text{blue-violet}}{[\mathrm{Ni}(\mathit{diam})_2(\mathrm{EtOH})_2]^{2+}} \underset{\text{cool}}{\overset{\text{heat}}{\rightleftharpoons}} \underset{\text{orange}}{[\mathrm{Ni}(\mathit{diam})_2]^{2+}} + 2\mathrm{EtOH} \tag{4}$$

However, the addition of a large amount of $NaClO_4$ makes the aqueous solution notably thermochromic due to the inert salt effect (Eq. (5)).

$$[\mathrm{Ni}(\mathit{diam})_2(\mathrm{H_2O})_2]^{2+} \underset{\text{cool}}{\overset{\substack{\mathrm{NaClO_4}\\ \text{heat}}}{\rightleftharpoons}} [\mathrm{Ni}(\mathit{diam})_2]^{2+} + 2\mathrm{H_2O} \tag{5}$$

The thermochromic properties of the nickel complex of 1,4-*bis*-(3-aminopropyl)-piperazine (*bapp*) have also been studied (Fig. 9) [32]. Interestingly, the piperazine ligand itself can only coordinate as a bidentate ligand in the chair form, but not in the boat form. When two (3-aminopropyl) groups are introduced to the piperazine

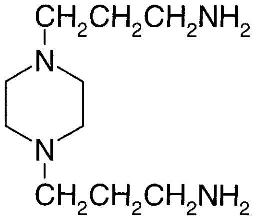

Fig. 9. Structure of 1,4-*bis*-(3-aminopropyl)-piperazine (*bapp*)

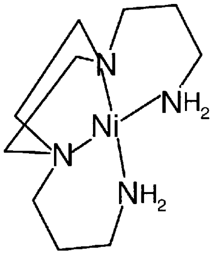

Fig. 10. Structure of $[\mathrm{Ni}(bapp)]^{2+}$

moiety, the resulting tetradentate *bapp* ligand can stabilize the piperazine skeleton in the boat conformation through coordination to a metal center.

In certain organic solvents (*DMF* and acetonitrile), the orange colour of $[\mathrm{Ni}(bapp)]^{2+}$ (Fig. 10) becomes blue upon cooling to *ca.* −50°C, indicating the formation of an octahedral species $[\mathrm{Ni}(bapp)(solv)_2]^{2+}$ at lower temperatures. When Cl^- or Br^- ions are present in such solutions, another thermochromic equilibrium (Eq. (6)) between the halide-containing 5-coordinated species and the original square-planar structure has been confirmed [33].

$$\begin{array}{ccc} [\mathrm{Ni}(bapp)]^{2+} + \mathrm{Cl}^- & \leftrightarrows & [\mathrm{Ni}(bapp)\mathrm{Cl}]^+ \\ \text{orange} & & \text{blue-violet} \\ \text{square planar} & & \text{5-coordinaed} \end{array} \tag{6}$$

Solvatochromism

Solvatochromism is defined as the pronounced change in position and sometimes intensity of an electronic absorption or emission band accompanying a change in the polarity of the medium. This can be even detected visually by the change of solution colour when going from one solvent to another.

Solvatochromism of mixed-ligand complexes

Mixed-ligand complexes of copper(II) or nickel(II) ions show a pronounced solvatochromism in solution. Extensive studies have been focused on mixed-ligand complexes containing N-alkylated diamines (*diam*) and β-diketonates (*dike*) of the general formula $[M(diam)(dike)]^+$ (Fig. 11) [34–38]. An interesting property of these complexes is their high solubility in various organic solvents due to increasing hydrophobic properties of the groups surrounding the central metal ion, *i.e.* the alkyl substituent groups on the *diam* and the *dike* ligands. The study has been extended to cover a series of different substituents on both ligands (Tables 3, 4).

According to different interactions between the solvent and the studied solute complex, solvatochromic behaviour can be classified into the following categories.

Perchlorate and tetraphenylborate mixed-ligand complexes (solute-solvent interactions)

Compounds of the type $[M(diam)(dike)]X(M = \mathrm{Cu(II)}$ or $\mathrm{Ni(II)}$, $X = \mathrm{ClO}_4^-$ or $\mathrm{BPh}_4^-)$ are of square-planar structure. These anions act only as counter ions and

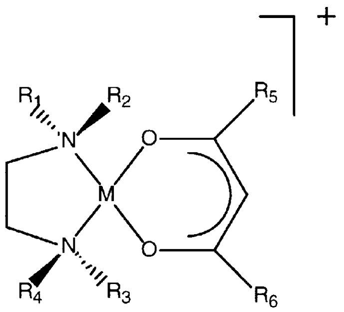

Fig. 11. Mixed-ligand complexes $[M(dike)(diam)]X$

Table 3. Diamine ligands with different substituents R^1–R^4

Ligand	Abbreviation	R^1	R^2	R^3	R^4
N,N,N′,N′-Tetramethylethylenediamine	*tmen*	Me	Me	Me	Me
N,N,N′,N′-Tetraethylethylenediamine	*teen*	Et	Et	Et	Et
N,N′-Dimethylethylenediamine	*sym-dmen*	Me	H	Me	H
N,N-Dimethylethylenediamine	*unsym-dmen*	Me	Me	H	H
N,N′-Diethylethylenediamine	*sym-deen*	Et	H	Et	H
N,N-Diethylethylenediamine	*unsym-deen*	Et	Et	H	H

Table 4. β-Diketonate ligands with different substituents R^5–R^6

Ligand	Abbreviation	R^5	R^6
Acetylacetonate	*acac*	Me	Me
Benzolylacetonate	*bzac*	Me	Ph
Dibenzoylmethanate	*dibm*	Ph	Ph
Trifluoroacetylacetonate	*tfac*	Me	CF_3
Hexafluoroacetylacetonate	*hfac*	CF_3	CF_3
Dipivaloylmethanate	*dipm*	*tert*-Bu	*tert*-Bu

do not interact with any solute (complex cation) in the solid state and in solution [39]. Therefore, the complex structure depends only on the donor properties of the solvent used (*Gutmann*'s donor number *DN*), and only solute-solvent interactions can be considered [40]. In a typically non-coordinating solvent (low *DN*) such as 1,2-dichloroethane (*DCE*), solutions of [Ni(*diam*)(*dike*)]*X* are diamagnetic and red in colour, whereas in highly coordinating solvents (high *DN*), such as *DMSO* or *DMF*, paramagnetic green or blue solutions are obtained (Eq. (7)).

$$\underset{\text{red}}{[\mathrm{Ni}(diam)(dike)]^+} + 2\,solv \leftrightarrows \underset{\text{blue or green}}{[\mathrm{Ni}(diam)(dike)(solv)_2]^+} \qquad (7)$$

Increasing donor ability of solvents shifts the equilibrium to the right. Substitutions on both $diam(R^1\text{-}R^4)$ and $dike(R^5\text{-}R^6)$ have a pronounced effect on the above equilibrium (Eq. (7)). Electron-donating substituents on *dike* shift the equilibrium to the left, whereas electron-withdrawing substituents favour the solvent coordination to the metal center and, consequently, shift the equilibrium to the right hand side. In other words, when R^5 and R^6 are electron-donating, the ligand field strength of *dike* is increased. The coordination sphere around the metal ion becomes electron-rich, which makes it difficult for a solvent molecule to approach the axial centres. The equilibrium constant K for the above reaction (Eq. (7)) was found to increase in the following order:

$$dipm < acac < bzac < dibm < tfac < hfac$$

Spectroscopic data show that the equilibrium constant decreases with increasing number and size of the alkyl groups on *diam*, obviously because of steric hindrance. The observed order of decreasing K is as follows [41]:

$$sym\text{-}dmen > unsym\text{-}dmen > sym\text{-}deen > tmen > unsym\text{-}deen > teen$$

Spectroscopic studies on [Cu(*diam*)(*dike*)]ClO_4 complexes in many non-aqueous solvents showed a good correlation between their d–d absorption maxima and the donor strength of solvent used [42]. Absorption peaks of complexes in inert solvents like *DCE* (low *DN*) were shifted to higher frequencies than in solvents with high *DN* such as *DMSO*.

Halide and pseudohalide mixed-ligand complexes (solute-solute-solvent interactions)

The behaviour of halide and pseudohalide complexes in various solvents is very different from that of the perchlorate compounds. The copper(II) complex [Cu(*diam*)(*dike*)*X*] is 5-coordinated (square-pyramidal), whereas the nickel(II) complex is a dinuclear, octahedral complex bridged by NCS^- ligands: [(*tmen*)(*acac*)Ni$(NCS)_2$Ni(*acac*)(tmen)]. In this review, the solution behaviour of the copper(II) complexes [Cu(*diam*)(*dike*)*X*] where $X = Cl^-$, Br^-, I^-, or NCS^- is discussed. In this case, both the anion X and the solvent molecule can coordinate to the copper(II) centre, and a competition of these two types of ligands at the axial sites of the chelate cation takes place (solute-solute-solvent interactions, Fig. 12). In

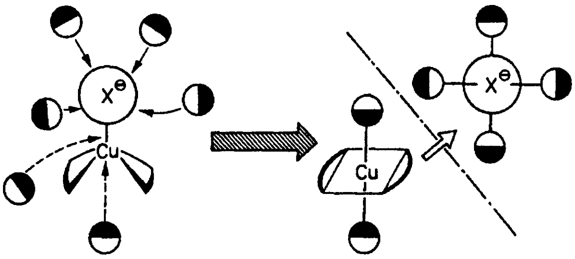

Fig. 12. Schematic representation of the dissociation of a 5-coordinated complex in a polar solvent; the solvent molecules are represented by balls; their white and black halves correspond to the positive and negative ends of the molecules, respectively

a polar solvent, the negative centre of the 5-coordinated complex, *i.e.* X, attracts the positive ends of solvent molecules. The Cu-X bond is weakened by this interaction, and finally the X anion, which is rather strongly solvated, dissociates off [38]. The main driving force of this reaction is the solvation power of the solvent as expressed by the acceptor number (*AN*) [43–45].

With two solvents of similar *AN*, that with higher *DN* will be favoured with respect to coordination to the metal centre. Solvent molecules pull out the anion X as acceptors, whereas as donors they solvate the complex cation. Therefore, a new polarity parameter [39, 46] of the solvent, the polarity factor P_f, is introduced as a linear combination of *AN* and *DN* (Eq. (8)).

$$P_f = a \times (AN) + b \times (DN) \tag{8}$$

Our results confirm the ease of anion (X) dissociation with increasing P_f in the order $I^- > Br^- > Cl^-$. In [Cu(*tmen*)(*dike*)X] complexes, the increasing strength of the Cu-X bond results in a stabilization of the 5-coordinated species which in turn is reflected in the decrease of its ν_{max}. In solvents of very low P_f (*DCE* or acetone), where the 5-coordinated species predominate, ν_{max} values increase following the order $I^- < Br^- < Cl^-$, thus indicating increasing stabilization of 5-coordinated species in the same order. The ν_{max} diagram of Cl- and Br-complexes with different kinds of *dike* in various solvents (Fig. 13) has been reported. In these complexes, ν_{max} changes in the order MeOH > EtOH > *DMSO* > *DMF* > *NM* > CH_3CN >

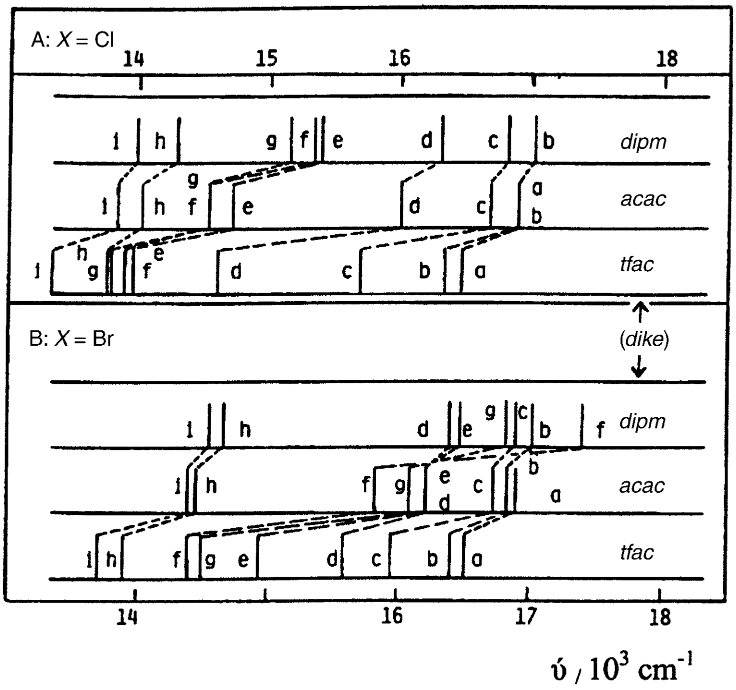

Fig. 13. ν_{max} values of the complexes [Cu(*tmen*)(*dike*)X] in various solvents; A: [Cu(*tmen*)(*dike*)Cl], B: [Cu(*tmen*)(*dike*)Br]; solvents from (a) to (i): H_2O (a), CH_3OH (b), C_2H_5OH (c), *DMSO* (d), *DMF* (e), CH_3NO_2 (f), CH_3CN (g), *DCE* (h), CH_3COCH_3 (i)

DCE ≅ acetone which is nearly the same order as that of P_f. In the same solvent, the change of ν_{max} with different *dike* moieties follows the order *dipm* > *acac* > *tfac* > *hfac*. This is in accordance with the ligand field strength of the *dike* ligands. The anion effect and substituent effect on *dike* may be called Axial Ligand Field Variation Effect and Equatorial Ligand Field Variation Effect, respectively. Owing to the latter effect, the tetragonal structure is stabilized, especially in the case of *dipm* chelates.

Nitrato and bis-(β-diketonato) mixed-ligand complexes

Two kinds of mixed-ligand complexes with octahedral geometry are involved in this case. The first complex contains a bidentate nitrato anion and is characterized by the general formula $[\mathrm{Ni}(diam)(dike)\mathrm{NO_3}]$. In the second one, $[\mathrm{Ni}(diam)(dike)_2]$, an additional *dike* ligand is introduced. In solvents of low *DN*, the nitrato complexes dissolve without structural changes to form non-conducting solutions. Solvents with higher *DN* displace the $\mathrm{NO_3^-}$ ligands, and the quilibrium described by Eq. (9) is established [47] which is accompanied by only minor spectroscopic variations [48, 49] due to the unchanged geometry.

$$\underset{\text{octahedral}}{[\mathrm{Ni}(diam)(dike)\mathrm{NO_3}]} + 2\,\mathrm{solv} \leftrightarrows \underset{\text{octahedral}}{[\mathrm{Ni}(diam)(dike)(solv)_2]^+} + \mathrm{NO_3^-} \qquad (9)$$

The octahedral $[\mathrm{Ni}(diam)(dike)_2]$ complexes dissolve in various kinds of organic solvents without structural and spectroscopic changes. The introduction of the additional *dike* shields the central metal cations effectively by three organic ligands with eight alkyl groups. As a result, these chelates are very soluble in non-polar organic solvents. The strong shielding effect also prevents solute-solute interactions, thus allowing to obtain pure crystals of such chelates by sublimation. A list of donor and acceptor numbers together with some other polarity parameters are collected in Table 5 [43, 44].

The behaviour of nickel complexes of the general formula $[\mathrm{Ni}(diam)(dike)X]$ $(X = \mathrm{BPh_4^-}, \mathrm{ClO_4^-}, \mathrm{NO_3^-}, dike)$ in various organic solvents is summarized in the following schematic diagram (Fig. 14) showing all possible structural changes induced by the polarity of the solvent (solvatochromism).

Mixed-ligand complexes as colour indicators for solvent polarity: an application of solvatochromism

The mixed-ligand complex $[\mathrm{Cu}(acac)(tmen)]\mathrm{ClO_4}$ is known to be solvatochromic owing to the structure changes caused by the solvation processes [34, 38]. The coordination centre which determines the position of the d–d band is extremely sensitive to nucleophilic solvent attack. This fact led to its use as a colour indicator for solvent polarity for *DN* values within the range of 5 to 30. However, anomalies appear in very weak or very strong donor solvents (Table 6). The λ_{max} value of this complex decreases with decreasing *DN* from pyridine to nitromethane; when the *DN* gets still smaller, however, it increases notably again. In such weak donor solvents λ_{max} becomes slightly concentration dependent [50]. Such problems have

Table 5. Donor numbers (*DN*), acceptor numbers (*AN*), dielectric constants (*D*), and dipole moments (μ/Debye) of various solvents at 25°C

Solvent	*DN*	*AN*	*D*	μ
Acetic acid (AcOH)		52.9	6.2	1.75
Acetic anhydride (Ac_2O)	10.5		20.7 (19°C)	2.82
Acetone (*Ac*)	17.0	12.5	20.7	2.86
Acetonitrile (*AN*)	14.1	18.9	36.0	3.44
Acetyl chloride	0.7		15.8	2.71
Benzene (*Bz*)	0.1	8.2	2.3	0.0
Benzonitrile (*BN*)	11.9	15.5	25.2	4.05
Benzyl cyanide	15.1		18.4 (27°C)	3.50
Chloroform ($CHCl_3$)	0.0	25.1	4.7	1.15
1,2-Dichloroethane (*DCE*)	0.0	16.7	10.1	1.75
Diethyl ether (Et_2O)	19.2	3.9	4.2	1.25
Dimethylformamide (*DMF*)	26.6	16.0	36.7	3.86
Dimethylsulfoxide (*DMSO*)	29.8	19.3	46.7	3.90
1,4-Dioxane (*diox*)	14.8	10.8	2.2	0.45
Ethanol (EtOH)	20.0	37.1	24.3	1.70
Ethyl acetate (EtOAc)	17.1	9.3	6.0	1.88
Hexane	0.0	0.0	1.9	0.0
Methanol (MeOH)	19.0	41.3	32.6	1.70
Nitrobenzene (*NB*)	4.4	14.8	34.8	4.03
Nitroethane (*NE*)			28.5	
Nitromethane (*NM*)	2.7	20.5	36.7	3.57
Pyridine (*Py*)	33.1	14.2	12.3	2.37
Tetrahydrofuran (*THF*)	20.0	8.0	7.4	1.75
Triethylamine (Et_3N)	61.0	1.4	2.4	0.79
Trimethyl phosphate (*TMP*)	23.0	16.3	20.6 (20°C)	
Water (H_2O)	18.0	54.8	78.4	1.84

been overcome by using [Cu(*acac*)(*tmen*)]BPh_4. UV/Vis spectra of this complex (Fig. 15) in various solvents of $DN > 5$ are very similar to those of the perchlorate, but the anomalies in very weak donor solvents are absent. The λ_{max} value continues to decrease with decreasing solvent basicity; this can be expressed in terms of *Schmid*'s DN_B [51, 52]. The deviation of the perchlorate complex at low DN_B is due to ion-pair formation, *i.e.* weak coordination of the perchlorate anion to the chelate plane. In case of tetraphenylborate, no effective ion-pair formation will occur since BPh_4^- is sterically demanding and inert. The regular spectroscopic trend therefore continues also in very weak donor solvents with no anomaly. In addition to the d–d band, the UV/Vis spectra of [Cu(*acac*)(*tmen*)]BPh_4 show a continuous background absorption in the blue part which seems to be the tail of a strong CT band in the near ultraviolet. With the decrease of *DN* or DN_B, this absorption is shifted towards red and overlaps remarkably with the d–d band in very weak donor solvents. The λ_{max} values of the d–d band in these solvents were corrected by assuming that d–d band has the same ν-symmetrical, *pseudo-Gaussian* shape as in other solvents.

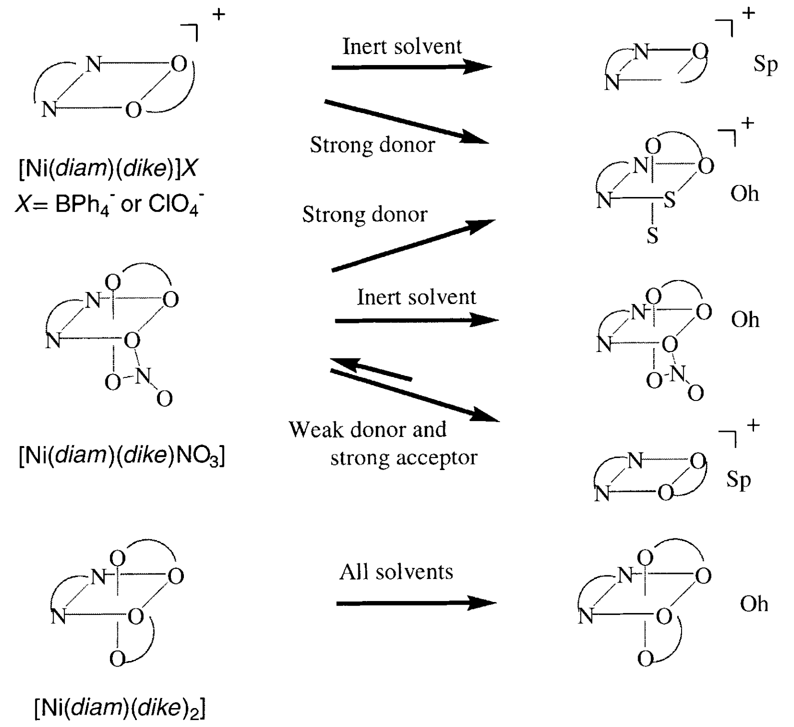

Fig. 14. Schematic diagram showing all possible structural changes of [Ni(*diam*)(*dike*)*X*] complexes resulting from solute-solute-solvent interactions

Table 6. Absorption maxima of the d–d band of [Cu(*acac*)(*tmen*)]*X* in various solvents

Solvent	λ_{max}/nm			DN/DN_B^a
	$X = ClO_4^-$	$X = BPh_4^-$		
		Observed	Corrected	
Dichloromethane $(10^{-2} M)$	550[c]	488	515	(1.2)
Chlorobenzene $(10^{-3} M)$	572[c]	480	520	(1.2)
1,2-Dichloroethane $(10^{-2} M)$	543[c]	498	520	(2.9)
Nitrobenzene $(10^{-3} M)$	533	490	522	(3.7)
Nitromethane	532	527	530	(4.8)
Acetonitrile	578	573		14.1
Acetone	571	569		17.0
Dimethylformamide	603	602		26.6
Pyridine $(10^{-1} M)$	624[b]	623[b]	613	33.1
2-Picoline $(10^{-2} M)$	624[b]	620[b]		

[a] DN_B in parentheses; [b]strongly concentration dependent; [c] slightly concentration dependent

Conclusions

Thermochromism of various nickel(II) complexes with cyclic diamines or their derivatives in solution is always accompanied by structural changes. Thermochromic colour changes caused by changes in the spin state are sometimes observed

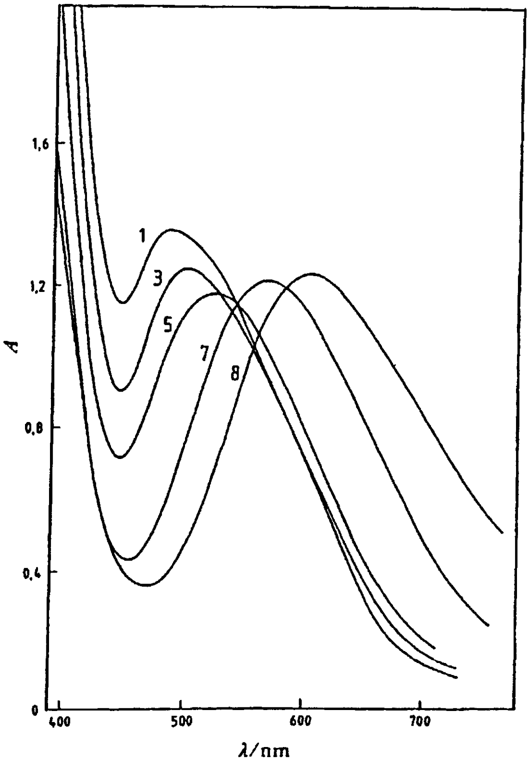

Fig. 15. UV/Vis spectra of [Cu(*acac*)(*tmen*)]BPh_4 in dichloromthane (1), 1,2-dichloroethane (3), nitromethane (5), acetone (7), and *DMF* (8)

in iron(II) complexes. Investigations on the solvatochromism of different chelates show how the colour changes can be used for the understanding of various polarity concepts in addition to studying their coordination structure.

Acknowledgements

This work was partly supported by a Grant-in-Aid (Scientific Research No. 11304046) from the Ministry of Education, Science, Culture, and Sports of Japan.

References

[1] Kahn O (1993) Molecular Magnetism. VCH, New York
[2] Toftlund H (1989) Coord Chem Rev **94**: 67
[3] Gütlich P, Hauser A, Spiering H (1994) Angew Chem **106**: 2109
[4] König E (1991) Struct Bonding **76**: 51
[5] Gütlich P (1981) Struct Bonding **44**: 83
[6] Deccurtins S, Gütlich P, Köhler CP, Spiring H, Hauser A (1984) Chem Phys Lett 1
[7] Deccurtins S, Gütlich P, Hasselbach KM, Hauser A, Spiring H (1985) Inorg Chem **24**: 2174
[8] Chum HL, Vanin JA, Holanda MID (1982) Inorg Chem **21**: 1146
[9] Addison AW, Burman S, Wahlgren CG (1987) J Chem Soc Dalton Trans 2621
[10] Renz F, Hasegawa M, Hoshi T, El-Ayaan U, Linert W, Fukuda Y (1999) Mol Cryst Liq Cryst **335**: 531

[11] Renz F, El-Ayaan U, Linert W, Fukuda Y (1999) Mol Cryst Liq Cryst **335**: 521
[12] Strauß B, Gutmann V, Linert W, Jameson RF (1992) Monatsh Chem **123**: 537
[13] Strauß B, Gutmann V, Linert W, Jameson RF (1993) Monatsh Chem **124**: 515
[14] Linert W, Konecny M, Renz F (1994) J Chem Soc Dalton Trans 1523
[15] Enamullah M, Linert W (1995) J Coord Chem **35**: 325
[16] Enamullah M, Renz F, El-Ayaan U, Wiesinger G, Linert W (1997) Vibr Spect **335**: 521
[17] Evans DF (1959) J Chem Soc 2003
[18] Beattie JK, McMahon KJ (1988) Aust J Chem **41**: 1315
[19] McGarvey JJ, Lawthers I, Heremans K, Toftlund H (1990) Inorg Chem **29**: 252
[20] McGarvey JJ, Lawthers I (1982) J Chem Soc Chem Commun 906
[21] Dose EV, Hoselton MA, Sutin N, Tweedle MF, Wilson LJ (1978) J Am Chem Soc **100**: 1141
[22] Bocá R, Baran P, Dlhán L, Šima J, Wiesinger G, Renz F, El-Ayaan U, Linert W (1997) Polyhedron **16**: 47
[23] Goodgame DML (1972) Bull Soc Chem Fr 3
[24] Sams JR, Scott JC, Tsin TB (1973) Chem Phys Lett **18**: 451
[25] Sams JR, Tsin TB (1976) J Chem Soc Dalton Trans 488
[26] Sasaki Y, Shigematsu T (1973) Bull Chem Soc Jpn **46**: 3438
[27] Reeder KA, Dose EV, Wilson LJ (1978) Inorg Chem **17**: 1071
[28] Miller JS (2000) Encyclopedia of Smart Materials. Wiley, New York
[29] Yamaki S, Fukuda Y, Sone K (1982) Chem Letters 269
[30] Fukuda Y, Miyamae H, Yamagata K, Sone K (1984) Chem Letters 1309
[31] Sone K, Fukuda Y (1987) Inorganic Thermochromism, Inorganic Chemistry Concepts, vol 10. Springer, Berlin Heidelberg
[32] Iwasaki N, Sone K, Fukuda Y (1975) Z Anorg Allg Chem **412**: 170
[33] Gibson JG, McKenzie ED (1971) J Chem Soc **A**: 1029
[34] Fukuda Y, Sone K (1972) Bull Chem Soc Jpn **45**: 465
[35] Fukuda Y, Shimura A, Mukaida M, Fujita E, Sone K (1974) J Inorg Nucl Chem **36**: 1265
[36] Fukuda Y, Miura Y, Sone K (1977) Bull Chem Soc Jpn **50**: 154
[37] Fukuda Y, Sato N, Hoshino N, Sone K (1981) Bull Chem Soc Jpn **54**: 428
[38] Sone K, Fukuda Y (1983) Ions and Molecules in Solution, Studies in Physical and Theoretical Chemistry, vol 27. Elsevier, Amsterdam, p 251
[39] Fukuda Y, Yasuhira M, Sone K (1985) Bull Chem Soc Jpn **58**: 3518
[40] Gutmann V (1967) Coord Chem Rev **2**: 239
[41] Nga NT, Fukuda Y, Sone K (1977) Bull Chem Soc Jpn **50**: 154
[42] Soukup RW, Schmid R (1985) J Chem Edu **62**: 459
[43] Gutmann V (1978) The Donor-Acceptor Approach to Molecular Interactions. Plenum Press, New York London
[44] Gutmann V (1968) Coordination Chemistry in Non-Aqueous Solutions. Springer, Vienna
[45] Mayer U (1983) Ions and Molecules in Solutions. Elsevier, Amsterdam, p 219
[46] Schmid R, Gutmann V (1982) Coord Chem Rev **43**: 150
[47] Fukuda Y, Sone K (1972) J Inorg Nucl Chem **34**: 2315
[48] Fukuda Y, Sone K (1975) J Inorg Nucl Chem **37**: 455
[49] Fukuda Y, Morishita R, Sone K (1976) Bull Chem Soc Jpn **49**: 1017
[50] Soukup RW, Sone K (1987) Bull Chem Soc Jpn **60**: 2286
[51] Schmid R (1983) J Sol Chem **12**: 135
[52] Schmid R, Sapunov VN (1982) Non-Formal Kinetics. VCH, Weinheim

Received April 2, 2001. Accepted (revised) April 19, 2001